

Digital Speckle Interferometry of Juno, Amphitrite and Pluto's Moon Charon

G. Baier, N. Hetterich and G. Weigelt, *Physikalisches Institut der Universität Erlangen, Fed. Rep. of Germany*

Introduction

The great advantage of Labeyrie's speckle interferometry (1970, *Astronomy and Astrophysics* **6**, 85) is its fascinating angular resolution. The resolution of conventional astrophotography is only about 1 arc second due to the atmosphere. Speckle interferometry yields 0.03 arc second in the case of a 3.6 m telescope or 0.08 arc second in the case of a 1.5 m telescope. The achievable resolution is independent of seeing. However, the limiting magnitude depends on seeing. At 2 arc second seeing we have achieved the limiting magnitude 16^m .

In this paper we will report digital speckle interferometry of the asteroids Juno (9^m) and Amphitrite (11^m) and of Pluto/Charon ($14^m/16^m$). In addition to these measurements we will briefly describe preliminary results of the Seyfert galaxy NGC 1068 (11^m), the quasar 3C273 (12.7^m) and the triple QSO PG 1115+080 (16.2^m). In a subsequent paper we will discuss the measurements in more detail. Also our first application of the speckle masking method, which yields high-resolution images instead of autocorrelations, will be discussed in a following report.

Photon-Counting Speckle Camera and Image Processing

Speckle interferometry essentially is a Fourier analysis of large numbers of *short-exposure photographs*, called speckle interferograms. The end result of the speckle interferometry process is the high-resolution autocorrelation of the object. For a 10^m -object about 10^3 speckle interferograms have to be processed, for a 14^m -object about 10^4 . Short exposures have to be used since only short exposures contain high-resolution information. The fine speckle structure, which is a random interferogram, carries the high-resolution information. Long exposures cannot be improved very much since in long exposures the fine speckle structure is washed out. The exposure time of speckle interferograms has to be $1/20$ sec or shorter in order to "freeze" the atmosphere. Due to this short exposure, image intensifiers have to be used. In our speckle camera we use a Varo tube with a gain of 300,000 or an EMI tube with a gain up to $3 \cdot 10^5$. For objects fainter than about 10^m we work in the photon-counting mode. Further parts of our speckle camera are a microscope for producing an effective focal length of about 100 to 500 m, interference filters, and a prism system to compensate for atmospheric dispersion. We use a 16-mm motion-picture camera to record the intensity-amplified speckle interferograms. Figs. 1a and 3a show various speckle interferograms. Individual speckles cannot be recognized since the objects are too faint. In the ESO *Messenger* No. 18, p. 25, speckle interferograms of brighter objects are shown.

Speckle Interferometry of the Asteroid Juno

For the measurement of the shape of Juno we have recorded and reduced 1,450 speckle interferograms of Juno and 555 speckle interferograms of a point source. Speckle interferograms of a point source are necessary to compensate the so-called transfer function of the speckle interferometry process. The speckle interferograms were recorded with the Danish

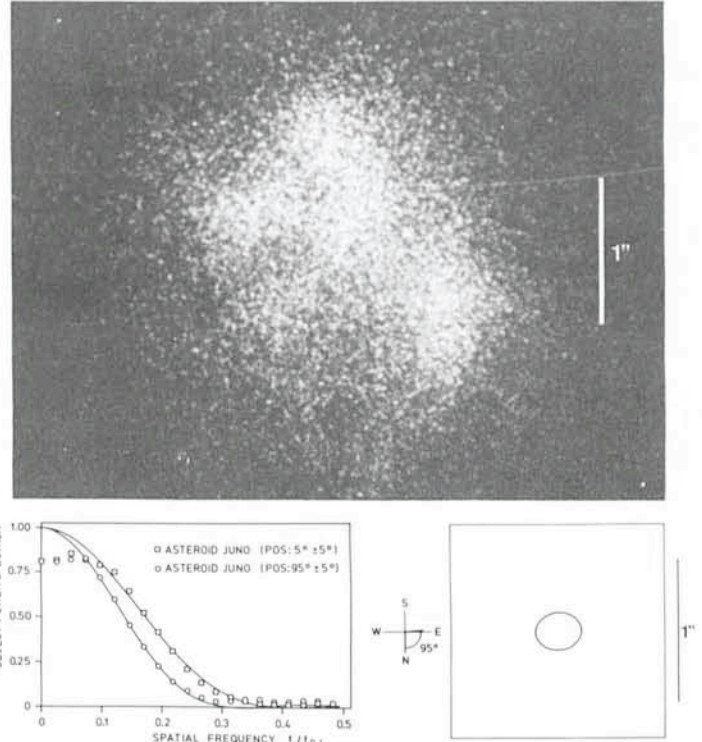


Fig. 1: Speckle interferometry of Juno.

- One of the 1,450 digitally reduced speckle interferograms.
- Radial plots of the object power spectrum for two different position angles.
- Calculated high-resolution shape of Juno (see text). The achieved resolution gain is a factor of about 20. We measured (epoch 24 Dec. 1979, $6^h 10^m$ U.T.): position angle of the long axis: $95^\circ \pm 5^\circ$; long axis: $288 \text{ km} \pm 20 \text{ km}$ ($0.32''$); short axis: $230 \text{ km} \pm 20 \text{ km}$ ($0.26''$). (From Juno/Amphitrite article submitted to *Astron. Astrophys.*)

1.5 m telescope. The exposure time per frame was $1/30$ sec; the seeing was about 2 arc second. Fig. 1a shows one of the speckle interferograms. We digitized all speckle interferograms with our digital TV-image-processing system (256×256 pixels per frame). The time-consuming part of the speckle interferometry process is the Fourier transformation of all speckle interferograms. We use a PDP 11/34 computer. The computing time is 32 sec per frame. The image processing steps of this experiment are described in more detail in our Juno/Amphitrite article, which has been submitted to *Astronomy and Astrophysics*. The speckle interferometry process yields the power spectrum or the autocorrelation of the object. Fig. 1b shows radial plots of the power spectrum of Juno for two different position angles. Fig. 1c is the resulting image of Juno calculated with the assumption of an elliptical shape and a homogeneous surface brightness.

Speckle Interferometry of the Asteroid Amphitrite

In the speckle interferometry experiment of Amphitrite we have recorded and reduced 1,776 speckle interferograms of Amphitrite and 755 speckle interferograms of an unresolvable

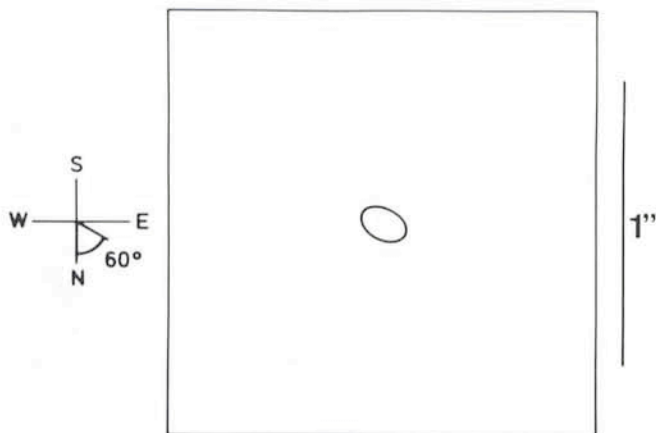


Fig. 2: Speckle interferometry of the shape of Amphitrite. Epoch: 4 April 1981, $8^{\text{h}}30^{\text{m}}$ U. T.; long axis: $255 \text{ km} \pm 30 \text{ km}$ ($0.17''$); short axis: $160 \text{ km} \pm 30 \text{ km}$ ($0.11''$); position angle of the long axis: $60^{\circ} \pm 20^{\circ}$. (From Juno/Amphitrite article submitted to Astron. Astrophys.)

star. The evaluation of the data consisted of the same steps as in the Juno experiment. Fig. 2 is the reconstructed image of Amphitrite calculated with the simplified assumption of an elliptical shape and a homogeneous surface. The power spectrum and the autocorrelation of Amphitrite show that Amphitrite has an elliptical shape at the achieved resolution of 0.08 arc second.

Digital Photon-Counting Speckle Interferometry of Pluto/Charon

We have measured Pluto/Charon in the nights of 2, 3 and 4 April 1981 with the Danish 1.5 m telescope. Fig. 3a shows one of the 15,000 recorded speckle interferograms. The exposure time was 1/20 sec per frame. Each speckle interferogram consists of about 50 photon events. In the case of such photon-counting data it is advantageous to use the following processing procedure, which was first proposed by A. Labeyrie et al. First the centres of gravity of all photons are calculated. Then the average autocorrelation of all interferograms is determined by calculating the histogram of the distances between all pairs of photon addresses. From this average autocorrelation the high-resolution object autocorrelation can be derived.

For the determination of the photon addresses we use a digital feedback loop in our image-processing system and a special pattern recognition algorithm. It is very impressive to observe on the computer monitor the shrinking of all photon dots to one pixel in about 1/5 sec. This fast pattern recognition algorithm is very flexible. It rejects ion events and scratches on film and it can separate photon pairs that are rather close.

Fig. 3 shows the Pluto/Charon measurements. Fig. 3a is one of the recorded speckle interferograms. Fig. 3b is the distribution of the photon addresses in Fig. 3a. Fig. 3c, 3d and 3e are the high-resolution autocorrelations of Pluto/Charon reconstructed from the speckle data of 2, 3 and 4 April 1981, respectively. In the time interval the autocorrelation peak of Charon moved about 41° around the central Pluto autocorrelation peak.

Photon-Counting Speckle Interferometry of the Extragalactic Objects NGC 1068, 3C273 and PG 1115+08

In addition to the measurements described in the preceding section, we have also performed speckle interferometry of

many spectroscopic double stars and of various extragalactic objects. These measurements will be described in one of the next issues of the *Messenger*. In the following text we will briefly describe some preliminary extragalactic results.

Seyfert Galaxy NGC 1068

We have recorded about 80,000 speckle interferograms of NGC 1068 at various wavelengths. Up to now, part of the H- α data have been reduced. These measurements show an elliptical cloud that has a size of about 0.5 arc second. Presently we are processing the data recorded at other wavelengths. We hope to find an unresolvable nucleus, the mysterious central engine.

QSO 3C 273

The reduction of 16,000 1.5 m speckle interferograms show that 3C 273 is smaller than 0.09 arc second, as expected.

QSO PG 1115+08

This famous quasar consists of three parts of magnitude 16.2^m, 18.1^m and 18.6^m, probably a gravitational lens effect. The 16^m-component is a double source with 0.5 arc second separation, first resolved by Hege et al. (1981, *Astrophysical Journal* **248**, L1). We have reduced 16,000 speckle interferograms recorded with the Danish 1.5 m and obtained exactly diffraction-limited resolution ($0.09''$) for the brightest component.

Image Reconstruction with the Speckle Masking Method

Speckle interferometry yields the high-resolution autocorrelation of the object. Direct images are usually not obtained. Therefore various authors have developed methods that yield direct images. One of these methods is the speckle masking method (1977, Weigelt, *Opt. Commun.* **21**, 55). We have applied speckle masking to speckle data recorded with the ESO 3.6 m telescope. The measurements yielded diffraction-limited images of many close spectroscopic binaries. The first image obtained is shown in our annual report 1982. We will publish some of these results in the next *Messenger* (with B. Wirtzner).

Speckle Spectroscopy

Another new method which we are currently developing is speckle spectroscopy (G. Weigelt, in: Proc. of the ESO Conf. on "Scientific Importance of High Angular Resolution at IR and Optical Wavelengths", Garching, 24–27 March 1981). This method yields images or autocorrelations of objective prism spectra with *very high angular resolution*, for example, 0.03 arc second in the case of a 3.6 m telescope. The raw data for this method are so-called spectrum speckle interferograms. In spectrum speckle interferograms each speckle is dispersed to a spectrum. For illustration Fig. 4 shows a spectrum speckle interferogram recorded in the laboratory. Similar images were also obtained with astronomical objects, but not with such nice colours. For actual speckle spectroscopy measurements the spectrum speckle interferograms are, of course, not recorded on colour film, but on black and white film and with a high-gain speckle camera. It is also necessary to use a restricted wavelength band instead of the whole visible spectrum. Speckle spectroscopy usually yields the autocorrelation of the high-resolution objective prism spectrum. If there is a point source near the object (less than about 5 arc second), then a direct image of the objective prism spectrum is obtained. There

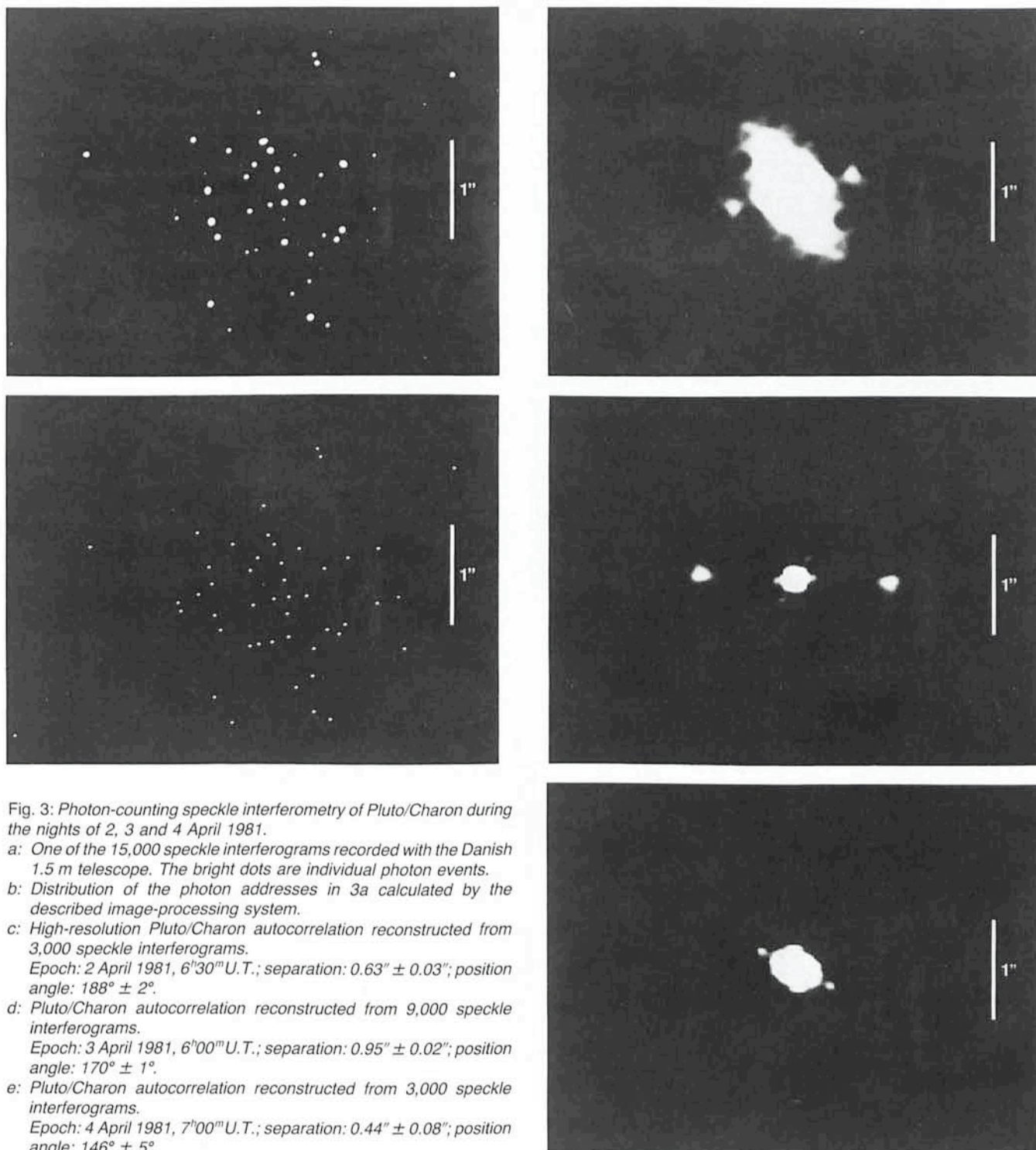


Fig. 3: Photon-counting speckle interferometry of Pluto/Charon during the nights of 2, 3 and 4 April 1981.

a: One of the 15,000 speckle interferograms recorded with the Danish 1.5 m telescope. The bright dots are individual photon events.

b: Distribution of the photon addresses in 3a calculated by the described image-processing system.

c: High-resolution Pluto/Charon autocorrelation reconstructed from 3,000 speckle interferograms.

Epoch: 2 April 1981, 6^h30^m U.T.; separation: 0.63" \pm 0.03"; position angle: 188° \pm 2°.

d: Pluto/Charon autocorrelation reconstructed from 9,000 speckle interferograms.

Epoch: 3 April 1981, 6^h00^m U.T.; separation: 0.95" \pm 0.02"; position angle: 170° \pm 1°.

e: Pluto/Charon autocorrelation reconstructed from 3,000 speckle interferograms.

Epoch: 4 April 1981, 7^h00^m U.T.; separation: 0.44" \pm 0.08"; position angle: 146° \pm 5°.

are several very interesting objects that are near a point source, for example R136a in the 30 Dor nebula, the discussed triple QSO and a few other quasars. Speckle spectroscopy can also be performed with the Space Telescope and the Faint Object Camera (see p. 106–108 in the above-mentioned paper). In the case of the Space Telescope there will be no problem to find a suitable point source in the isoplanatic neighbourhood of the object.

Conclusion

We have described speckle interferometry measurements of asteroids and of Pluto/Charon on three different nights. With

the developed photon-counting image-processing technique we are now reducing speckle data of extragalactic objects. For NGC 1068, 3C273 and PG 1115+08 we have already obtained results. With 16,000 frames per object we have achieved the limiting magnitude 16^m at 2 arc second seeing. This means that 20^m can be achieved with larger numbers of speckle interferograms and better seeing. 20^m is also the number that was already predicted by A. Labeyrie in 1973.

Acknowledgements

We wish to thank A. W. Lohmann for numerous helpful discussions, the German Science Foundation (DFG) for

financing the project and the staff members at La Silla for their assistance during the observations.

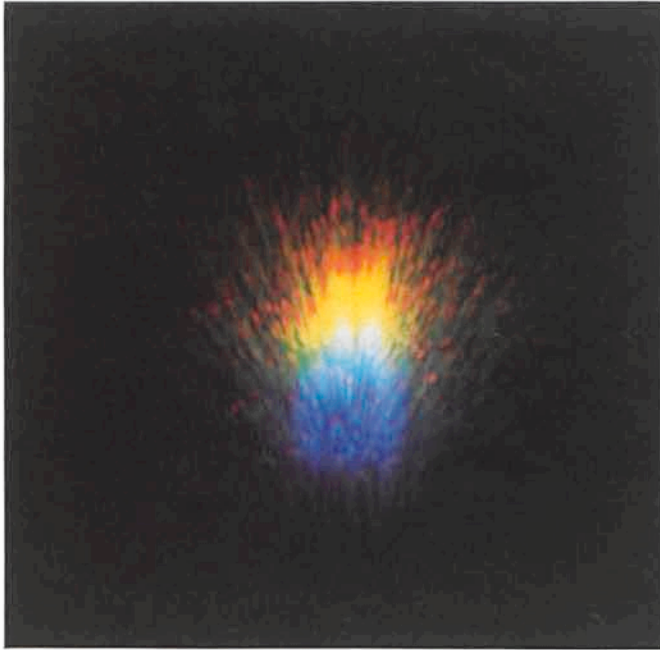


Fig. 4: Colour photographs of a laboratory spectrum speckle interferogram (see text). The laboratory speckles are produced by special phase distortion plates and the dispersion by a prism.

The CCD on La Silla

H. Pedersen and M. Cullum, ESO

Introduction

Throughout the history of observational astronomy, there has been a continual demand for detectors of higher sensitivity and lower noise. The ultimate goal, of course, is for an imaging detector that will record every photon reaching it with a noise level limited only by the random fluctuations of the photons themselves. Although we may not yet have the ideal detector, there has been a quiet revolution taking place in astronomy over the last year or so which has caused the world's major observatories to replace many of their older detectors, such as image intensifiers, by Charge-Coupled Devices (or CCDs as they are universally known).

The CCD

About as big as a fingernail, a CCD does not look particularly impressive: a rectangular piece of black silicon somewhat like a small solar cell. But, unlike the power-generating device, the surface of the CCD is divided into a vast number of small, discrete, light-sensitive elements or pixels. The size of these pixels is between 15 and 30 microns across, and the largest CCDs currently made have 640,000 such pixels. Even larger ones are on the drawing board. The CCD chips in use at La Silla at the present time have some 160,000 pixels covering a total field of about $10 \times 15 \text{ mm}^2$. CCDs were originally developed by the micro-electronic industry for television applications, but it did not take long for astronomers to discover them and fall in love with them. Their cherished characteristics include a very high sensitivity (responsive quantum efficiency exceeding

80% has been reported in the 600–700 nm range), linearity, low noise and excellent stability.

The entire surface of the CCD is traversed by rows of transparent electrodes of polycrystalline silicon. By applying a pattern of voltages to these electrodes, a series of potential wells is formed in the underlying silicon. Charge is prevented from spreading laterally along these wells by orthogonal potential barriers diffused into the silicon thus forming a matrix of individual charge-collecting centres. During an integration, electrons liberated by absorbed photons collect at these centres as indicated in Fig. 1a. This shows the potential well structure along the column of a three-phase CCD such as currently used at La Silla. The charge can be moved along the columns by varying the potential of the electrodes cyclically (Figs. 1b and 1c) so that the potential wells, and therefore the packets of accumulated charge, move along like a file of marching soldiers. At the end of an integration, the image is read out, first by shifting the entire charge-image down by one row, so that the bottom row is emptied into a "horizontal" output register, and then reading this register out serially to an output amplifier in the same way. This process is repeated, row by row, until the entire charge-image is cleared from the CCD. The output signals, after being processed and digitized, are transferred to computer mass-storage ready for display, reduction and analysis.

To minimize the accumulation of thermally generated charges during an integration, the CCD is cooled to a temperature of around 150 K. At this temperature, the dark current is negligible for most applications, and integration times of several hours are possible when the sky brightness permits. For reasons of cooling, as well as to avoid the risk of ice forming on the chip and to insulate it thermally from the surroundings, the CCD is mounted inside a vacuum cryostat.

The CCD on the Danish 1.5 m Telescope

The first CCD system to be permanently installed at La Silla was put into operation in June 1981 on the Danish 1.5 m telescope for direct imaging. The initial observations turned out to be so successful that several observers who had originally been scheduled for other instruments had second thoughts

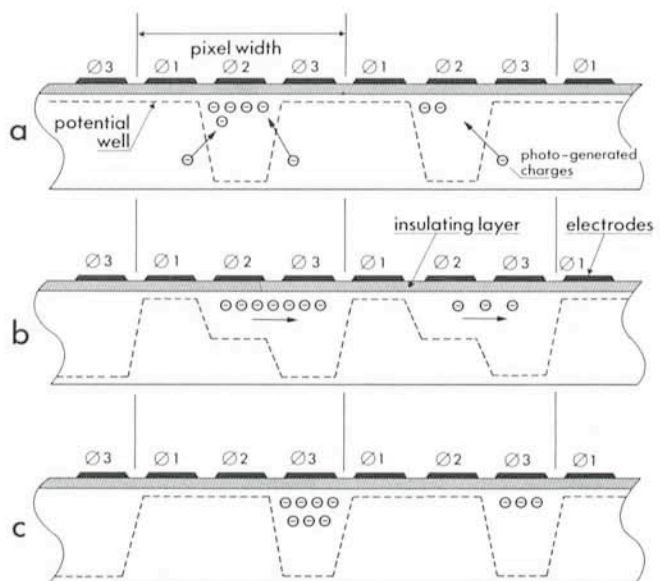


Fig. 1: Potential well structure generated by the overlaying electrodes along a column of a 3-phase CCD. (a) Static potential wells during integration; (b) and (c) charge transfer wells during image read-out.